

Do Two Different Reaction Mechanisms Contribute to the Hydroxylation of Primary Amines by Cytochrome P450?

Patrik Rydberg* and Lars Olsen

Department of Medicinal Chemistry, Copenhagen University, Universitetsparken 2, DK-2100 Copenhagen, Denmark

 Supporting Information

ABSTRACT: Three possible mechanisms have been suggested for the hydroxylation of primary and secondary amines by the cytochrome P450 enzyme family. We show that for the hydroxylation of primary alkyl amines, both the hydrogen abstraction and rebound mechanism and the direct oxygen transfer mechanism can contribute to the formation of the hydroxylated product. We also show that in the hydrogen abstraction and rebound mechanism the rebound step has higher activation energy than the hydrogen abstraction step, which is the opposite of the hydroxylation of aliphatic carbon atoms.

INTRODUCTION

Many primary amines have been shown to undergo amine hydroxylation in cytochromes P450.¹ Hence, knowledge of the hydroxylation mechanism and the rate limiting step is of vital importance for reactivity-based models that predict CYP mediated drug metabolism. Our model substrate, propan-2-amine, is a fragment of amphetamine and mexiletine, which both undergo amine hydroxylation.^{2,3} The hydroxylation of primary and secondary amines is also the first step in the formation of nitrones,⁴ which can cause the inhibition of cytochromes P450s by the formation of a bond between the nitrone nitrogen atom and the heme iron atom.⁵

During the past decade, the reaction mechanisms of reactions performed by the cytochrome P450 (CYP) enzyme family have been clarified by experimental and quantum chemical studies one by one,^{6,7} but there are still many mechanisms that have not been studied in great depth. In this study, we investigate the possible mechanisms for hydroxylation of primary amines using density functional theory (DFT) for the first time.

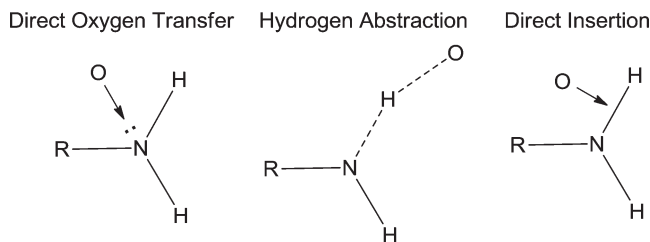
Three possible reaction mechanisms have been suggested for the hydroxylation of primary and secondary amines,⁸ and these are shown in Scheme 1: direct oxygen transfer (addition of the oxygen to the nitrogen lone pair followed by a rearrangement of the formed N-oxide into the hydroxylamine), hydrogen abstraction from the nitrogen followed by a rebound step, and direct insertion of the oxygen into the N-H bond. We have investigated the three mechanisms by performing DFT calculations on a porphine model system with propan-2-amine as a substrate.

COMPUTATIONAL METHODOLOGY

All calculations were performed with the Turbomole software package,⁹ version 6.1. In the calculations, compound I in the CYPs is modeled by a reduced heme model without side chains, iron porphine with SCH_3^- , and O^{2-} as axial ligands.

All calculations were performed using the B3LYP functional^{10–12} with the VWN(V) correlation functional¹³ (unrestricted formalism for open shell systems). The geometry optimizations, frequency calculations, and solvent calculations were performed

Scheme 1. The Three Mechanisms Suggested for the Hydroxylation of Primary and Secondary Amines



with the double- ζ basis set of Schäfer et al.,¹⁴ enhanced with a p function with the exponent 0.134915, on the iron atom, and the 6-31G(d) basis set^{15–17} for the other atoms. The final energies were determined by single point calculations using the 6-311+G(2d,2p) basis set^{18,19} for all atoms, except iron, for which we used the double- ζ basis set of Schäfer et al.,¹⁴ enhanced with s , p , d , and f functions (exponents of 0.01377232, 0.041843, 0.1244, 2.5, and 0.8; two f functions).²⁰

Solvent calculations were carried out with the continuum conductor-like screening model (COSMO),²¹ using an effective dielectric constant (ϵ) of 4 (except where otherwise mentioned). For the atomic radii, we used the optimized COSMO radii in Turbomole⁹ (and 2.0 Å for Fe).

All energies presented have been computed using the large basis set and include zero point vibrational corrections and solvation effects except where otherwise mentioned.

The barrier for the transformation of the direct oxygen transfer product (P^{Ox}) into the hydroxylated product (P^{Ha}) was computed using a propan-2-amine molecule and three water molecules (two of the water molecules created a proton transfer chain moving a proton from the nitrogen atom to the oxygen atom).

The hydrogen bond strength of nitrogen and carbon radicals to the hydroxyl group in the intermediate in the hydrogen

Received: June 20, 2011

Published: September 13, 2011

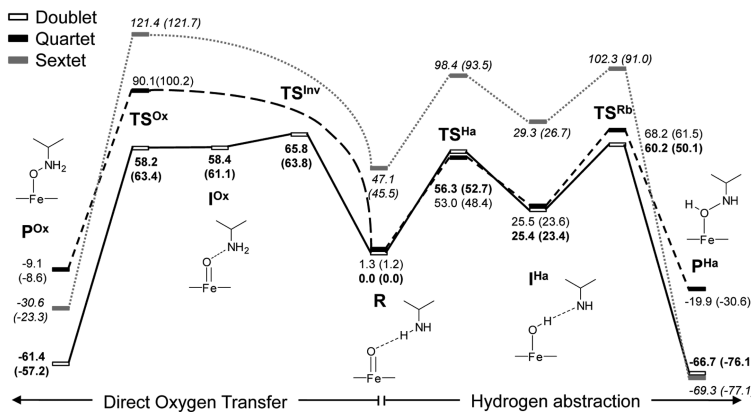


Figure 1. Energies for the direct oxygen transfer and hydrogen abstraction mechanisms for the doublet (bold text), quartet, and sextet (italic text) spin states in kilojoules per mole. Energies are from single-point calculations with the large basis set and include zero-point vibrational energies and solvent corrections computed with a dielectric constant of 4. The energies in parentheses are vacuum energies without solvent corrections.

abstraction mechanism were computed using model systems consisting of a water molecule and either an NH₂ radical or a CH₃ radical, with the 6-31G(d) basis set.^{15–17}

Spin densities were computed by Mulliken population analysis of the single-point calculations of the large basis set combination.

■ RESULTS AND DISCUSSION

The direct insertion mechanism has been shown to be unlikely for primary alkylamines,²² and later work has suggested that this mechanism should be more probable for nitrogen atoms with a highly delocalized lone pair.⁸ Our results support that the insertion mechanism is very unlikely for primary alkyl amines. Extensive work was done to find the transition state of this mechanism, starting from several different structures and using different reaction coordinates. However, each time we tried to locate the transition state for the insertion mechanism, the optimization ended up in structures belonging to either the direct oxygen transfer mechanism or the hydrogen abstraction mechanism. Hence, this mechanism will not be discussed any further.

The direct oxygen transfer mechanism has previously been studied for tertiary amines in the doublet and quartet spin states.^{23–26} In this work, we also study the mechanism in the sextet spin state. The transition state of the oxidation (TS^{Ox}) is quite similar to the results for the tertiary amine trimethylamine,²³ with a high barrier of 90 kJ/mol for the quartet spin state and a lower barrier of 58 kJ/mol for the doublet spin state (see Figure 1). In the sextet spin state, the barrier is even larger than in the quartet spin state (121 kJ/mol). This large energetic difference occurs because in the doublet spin state the two accepting orbitals to which the electrons from the nitrogen lone pair are transferred (one on the oxy group and one shared by the porphyrin ring and the cysteine sulfur atom) are singly occupied by electrons with opposite spin, and hence they can accept both the electrons in a straightforward manner. However, in the quartet (and sextet) spin states these orbitals are occupied by electrons with the same spin, and one of the electrons must either flip spin or end up in another orbital (an unoccupied iron 3d orbital), as has been shown previously for both nitrogen oxidation²³ and sulfur oxidations.^{7,23} While the spin density distributions basically are the same in propan-2-amin and trimethylamine, the structures have one difference:

the iron–oxygen–amine nitrogen angle is smaller for propan-2-amine due to weak interactions between an amine hydrogen atom and two of the nitrogen atoms in the porphyrin ring (structures and spin densities of the direct oxidation mechanism are shown in Figure 2). The major difference is that for propan-2-amine there is a requirement for an additional inversion step to get from the reactant state (R) to the direct oxidation transition state (TS^{Ox}). This step is required to move the nitrogen lone pair toward the oxygen, since it points away from the iron-bound oxygen atom in the reactant state (R) where there is a hydrogen bond between the iron-bound oxygen atom and one of the amine hydrogen atoms. The transition state of this nitrogen inversion (TS^{Inv}) is quite similar to the following intermediate and oxidation transition state with regard to spin densities (see Figure 2). However, the normal mode of the imaginary vibration is almost a pure nitrogen inversion in which the nitrogen atom is moving toward the oxygen atom (the structure distorted along the normal mode is shown in Figure S1, Supporting Information). While the intermediate (I^{Ox}) in the doublet state has a slightly higher energy than the transition state (0.2 kJ/mol), this is only due to solvation effects, because without these the intermediate (I^{Ox}) is lower in energy by 2.3 kJ/mol. Stable structures of this intermediate and the inversion transition state do not exist in the quartet or sextet spin states. This seems to be due to the high barrier of the direct oxidation in these spin states; what should have been the inversion transition state (TS^{Inv}) only shows up as a shoulder on scans of the oxygen nitrogen distance, because at this iron–oxygen distance the energy of the direct oxidation process is already quite high.

The rearrangement of the product of the direct oxygen transfer into the hydroxylated nitrogen (the product of the hydrogen abstraction and rebound reaction) in water has a lower barrier than either of the two reaction paths (18.3 kJ/mol). Hence, the direct oxidation product will be rearranged into the hydroxylated product more rapidly than it is formed, making the product of the direct oxidation unlikely to be observed in experiments.

The hydrogen abstraction and rebound mechanism has previously been studied extensively for the hydroxylation of aliphatic carbon atoms,⁶ and the hydrogen abstraction from the hydroxyl oxygen in ethanol has also been studied.²⁷ Since the hydrogen abstraction from nitrogen should be similar to the hydrogen abstraction from oxygen, we compare our results primarily to the

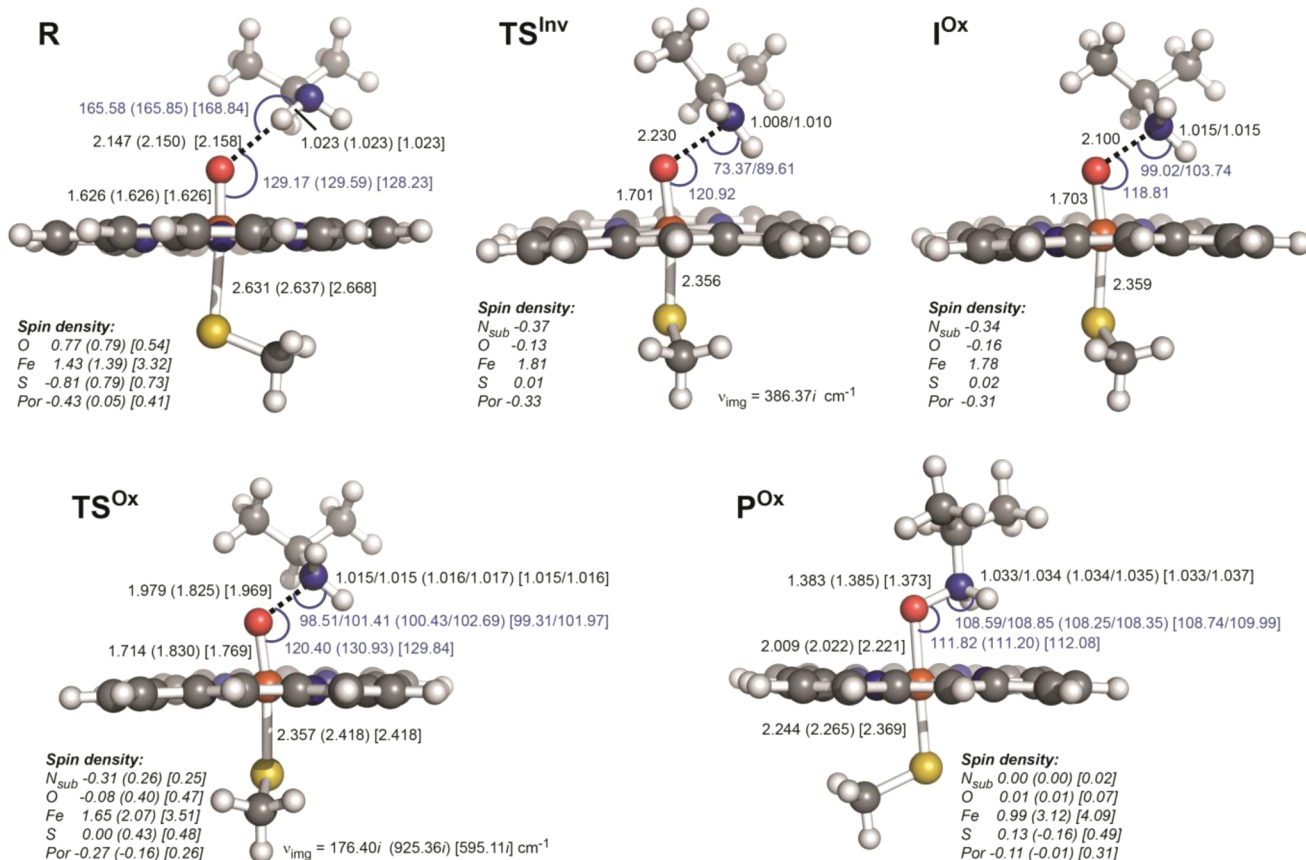


Figure 2. Structures, imaginary frequencies, geometrical features, and spin densities for the direct oxidation pathway. All data are shown as doublet (quartet) [sextet]. Distances in Ångströms are shown in black, and angles in degrees are shown in blue.

ones of Wang et al.,²⁷ who studied hydrogen abstraction from both oxygen and carbon atoms in ethanol.

The different states in the hydrogen abstraction and rebound mechanism are in general structurally similar to the results on ethanol,²⁷ but due to the formation of hydrogen bonds of different strengths by oxygen and nitrogen atoms compared to a carbon atom there are some significant differences. In the doublet spin state, the hydrogen abstraction transition state (TS^{H_a}) in propan-2-amine has an O–H distance which is similar to that for the hydrogen abstraction from carbon but longer than the one for hydrogen abstraction from oxygen, while the H–N distance is $\sim 0.1 \text{ \AA}$ shorter than the same H–C/O distances. In the quartet spin state, the O–H distance is intermediate between the corresponding distances in C/O hydrogen abstraction. Energetically, the hydrogen abstraction barrier is similar for all three reactions in both doublet and quartet spin states (49–56 kJ/mol). Since the study by Wang et al.²⁷ did not use the same model system and basis set as we do in this study, the differences in energies are most likely not significant. Earlier work has shown that changing the model system can change the activation energies of P450 mediated reactions by roughly 5 kJ/mol (our SCH_3^- model giving higher energies), but geometrically, the only significant change is in the iron–sulfur bond distance.²³ The sextet spin state is geometrically quite similar to the quartet spin state, but energetically it is much higher throughout the abstraction and rebound mechanism (with the exception of the product state). For the optimization of the intermediate structure (I^{H_a}) in the sextet spin state, the iron–sulfur bond had to be constrained to

generate a stable structure. The intermediates (I^{H_a}) are also structurally very similar with the exception of the distance between the oxygen bound hydrogen atom and the amine nitrogen radical (1.9 \AA , see Figure 3) which is intermediate between the corresponding distances in the hydrogen abstraction from oxygen (1.8 \AA) and carbon (2.0 \AA) atoms.²⁷ This strong nitrogen–hydrogen interaction causes the following rebound step to be quite different in the amine hydroxylation compared to the same step in the hydroxylation of aliphatic carbon atoms. Whereas the largest activation energy for the rebound step in the hydroxylation of the aliphatic carbons is only 13 kJ/mol higher than the intermediate (quartet spin state in the hydroxylation of camphor),²⁸ the lowest corresponding energy for the amine hydroxylation is 35 kJ/mol (TS^{R_b} , doublet spin state). This is also evident from the structure of the rebound transition state which shows a much later transition state with a shorter O–N distance compared to the corresponding transition state in the aliphatic carbon hydroxylation in camphor.²⁸ The reason for this high barrier in the rebound step is that the mechanism is actually slightly different compared to the rebound step in the hydroxylation of aliphatic carbon atoms. In the hydroxylation of aliphatic carbon atoms, the intermediate step (I^{H_a}) with a carbon radical has the radical oriented toward the hydroxyl group, and there is only one possible orientation. However, in the hydroxylation of nitrogen atoms, the radical on the nitrogen atom is actually almost perpendicular to the direction of the hydroxyl group, and the lone pair is interacting with the hydroxyl hydrogen atom, as shown in Scheme 2. This different orientation forces the

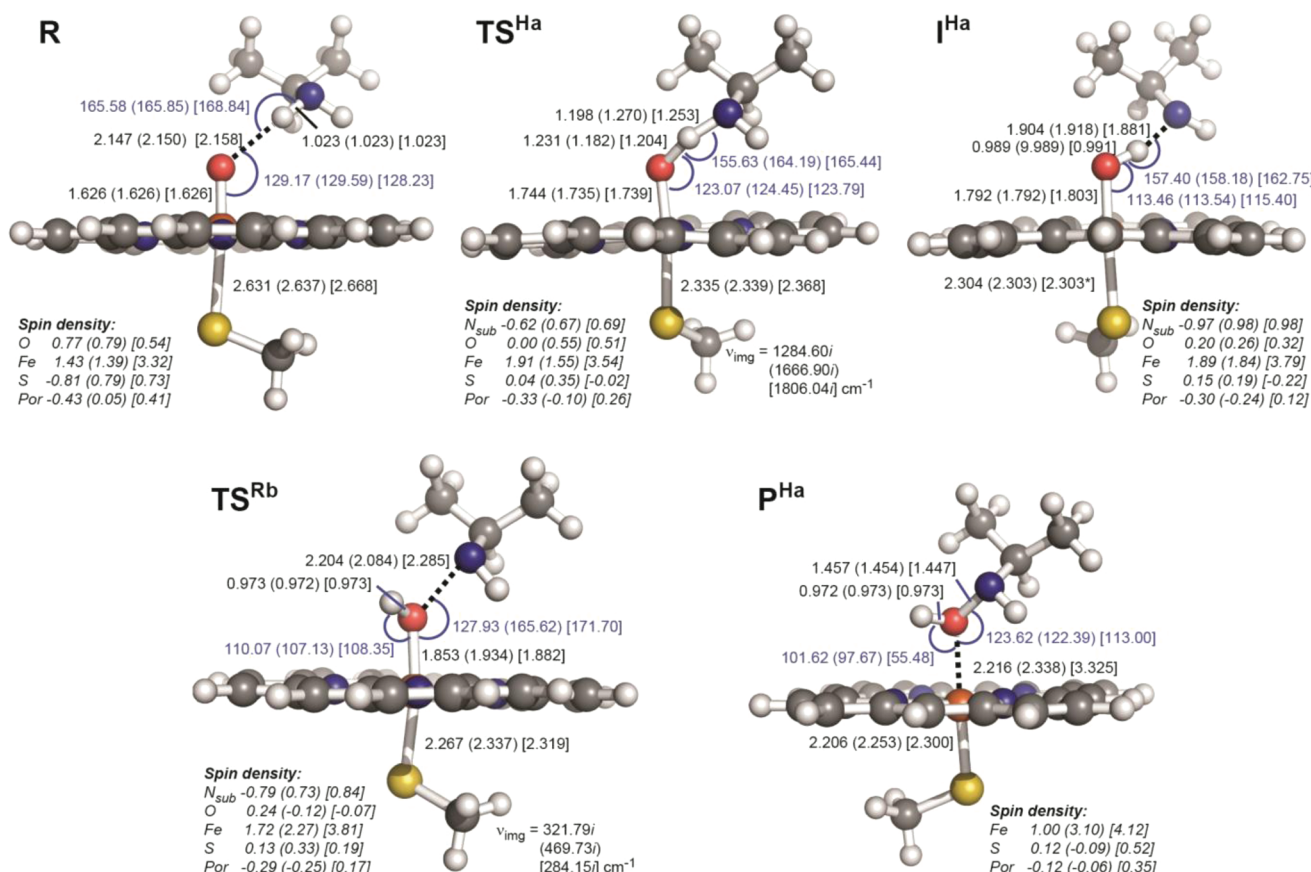
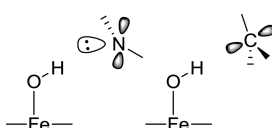


Figure 3. Structures, imaginary frequencies, geometrical features, and spin densities for the hydrogen abstraction and rebound pathway. All data are shown as doublet (quartet) [sextet]. Distances in Ångströms shown in black and angles in degrees shown in blue. The distance that was constrained during geometry optimization of the intermediate (I^{Ha}) in the sextet spin state is labeled with *. The reactant state (**R**) is identical to the one in Figure 2.

Scheme 2. The Different Radical Distributions in the Hydrogen Abstraction Intermediate for Amines and Aliphatic Carbons



system into an electronic reorganization during the rebound step, since the radical and the lone pair of the nitrogen have to change places. There is also a significant difference in hydrogen bond strength of the carbon and nitrogen radicals, which is another reason for the higher rebound barrier. The nitrogen radical has a 16 kJ/mol stronger hydrogen bond ($N \cdots H-O$) than the corresponding bond for a carbon radical. This hydrogen bond has to be broken during the rebound since the hydroxyl group has to be rotated to allow the oxygen lone pair to bind to the amine nitrogen. The barrier of the rebound transition state (TS^{Rb}) in the amine hydroxylation has an energy that actually is higher than the one for the hydrogen abstraction transition state (TS^{Ha}) for all three spin states. This is quite different from the same mechanism in the hydroxylation of aliphatic carbon atoms, where the doublet spin state rarely has a rebound barrier, while it is more common in the quartet spin state.²⁹ Still, even when there is a barrier for the rebound of aliphatic carbons, its

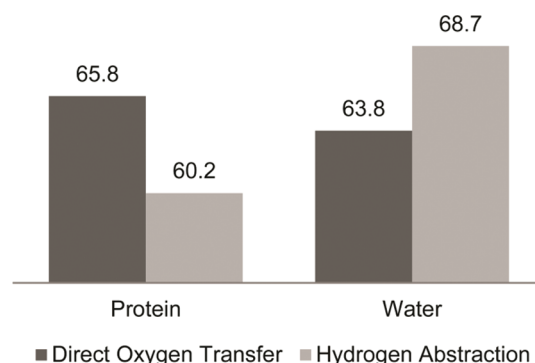


Figure 4. Comparison of the highest energies of the direct oxygen transfer and hydrogen abstraction mechanisms for solvation effects computed with water ($\epsilon = 80$) or in a protein ($\epsilon = 4$; energies in kJ/mol). The additional solvation effects of water make the direct oxygen transfer mechanism more favorable than the hydrogen abstraction mechanism.

energy is always much lower than the one for the hydrogen abstraction.

While the reaction energies show that the hydrogen abstraction mechanism is slightly more favorable than the direct oxygen transfer mechanism, this preference changes if we mimic water solvation by increasing the dielectric constant in our implicit

solvent model from 4 to 80 (see Figure 4). This indicates that explicit hydrogen bonds to the amine could change the preference to a direct oxygen transfer mechanism.

To investigate whether interactions with amino acids or water molecules are likely to contribute to the *N*-hydroxylation of primary amines, we investigated how the amine group in mexiletine interacts with amino acids in the active site of CYP1A2 when it is positioned in a way favorable for *N*-hydroxylation. To do this, we analyzed our docking results from a previous study,³⁰ and it is clear that there are no direct interactions between the amine group and any amino acids. Hence, interactions with water molecules which could exist in the active site would be required to shift the balance between the two mechanisms for the amine hydroxylation of mexiletine by CYP1A2.

CONCLUSIONS

The results of this study show that hydroxylation of primary alkyl amines (and probably also secondary alkyl amines) could undergo hydroxylation by cytochromes P450 either through a hydrogen abstraction and rebound mechanism or through the direct oxygen transfer mechanism, depending on the interactions between the substrate and water molecules or amino acids in the active site in each case.

There is one major difference in the hydrogen abstraction and rebound mechanism for hydroxylation of primary amines compared to the previously extensively studied hydroxylation of aliphatic carbon atoms, and that is the rebound step. Our results show that the radical intermediate has a different radical distribution in primary amines compared to aliphatic carbon atoms, resulting in a much stronger hydrogen bond in the intermediate and a much higher barrier for the rebound step. The barrier for the rebound step is even higher than the one for the hydrogen abstraction step in the hydroxylation of propan-2-amine.

ASSOCIATED CONTENT

Supporting Information. Coordinates for all structures mentioned in the text. Full data for the rearrangement of the product of direct oxygen transfer into the *N*-hydroxylated product. Tables with energies for all structures. Figure of the distortion along the normal mode for the inversion transition state. This material is available free of charge via the Internet at <http://pubs.acs.org>.

AUTHOR INFORMATION

Corresponding Author

*Phone: (+45) 35 33 61 62. Fax: (+45) 35 30 60 40. E-mail: pry@farma.ku.dk.

ACKNOWLEDGMENT

This work was supported by grants from the Danish medical research council and Lhasa Limited.

REFERENCES

- (1) Hlavica, P. N-oxidative transformation of free and N-substituted amine functions by cytochrome P450 as means of bioactivation and detoxication. *Drug Metab. Rev.* **2002**, *34*, 451–477.
- (2) Florence, V. M.; Distefano, E. W.; Sum, C. Y.; Cho, A. K. The Metabolism of (R)-(-)-Amphetamine by Rabbit Liver-Microsomes - Initial Products. *Drug Metab. Dispos.* **1982**, *10*, 312–315.
- (3) Labbe, L.; Abolfathi, Z.; Lessard, E.; Pakdel, H.; Beaune, P.; Turgeon, J. Role of specific cytochrome P450 enzymes in the N-oxidation of the antiarrhythmic agent mexiletine. *Xenobiotica* **2003**, *33*, 13–25.
- (4) Bondon, A.; Macdonald, T. L.; Harris, T. M.; Guengerich, F. P. Oxidation of Cycloalkylamines by Cytochrome-P-450 - Mechanism-Based Inactivation, Adduct Formation, Ring Expansion, and Nitrene Formation. *J. Biol. Chem.* **1989**, *264*, 1988–1997.
- (5) Murray, M. Drug-mediated inactivation of cytochrome P450. *Clin. Exp. Pharmacol. Physiol.* **1997**, *24*, 465–470.
- (6) Shaik, S.; Kumar, D.; de Visser, S. P.; Altun, A.; Thiel, W. Theoretical perspective on the structure and mechanism of cytochrome P450 enzymes. *Chem. Rev.* **2005**, *105*, 2279–2328.
- (7) Shaik, S.; Cohen, S.; Wang, Y.; Chen, H.; Kumar, D.; Thiel, W. P450 Enzymes: Their Structure, Reactivity, and Selectivity-Modeled by QM/MM Calculations. *Chem. Rev.* **2010**, *110*, 949–1017.
- (8) Nishida, C. R.; Knudsen, G.; Straub, W.; de Montellano, P. R. O. Electron supply and catalytic oxidation of nitrogen by cytochrome P450 and nitric oxide synthase. *Drug Metab. Rev.* **2002**, *34*, 479–501.
- (9) Klamt, A.; Jonas, V.; Burger, T.; Lohrenz, J. C. W. Refinement and parametrization of COSMO-RS. *J. Phys. Chem. A* **1998**, *102*, 5074–5085.
- (10) Becke, A. D. Density-Functional Exchange-Energy Approximation with Correct Asymptotic-Behavior. *Phys. Rev. A* **1988**, *38*, 3098–3100.
- (11) Lee, C. T.; Yang, W. T.; Parr, R. G. Development of the Colle-Salvetti Correlation-Energy Formula Into A Functional of the Electron-Density. *Phys. Rev. B* **1988**, *37*, 785–789.
- (12) Becke, A. D. Density-Functional Thermochemistry. III. The Role of Exact Exchange. *J. Chem. Phys.* **1993**, *98*, 5648–5652.
- (13) Vosko, S. H.; Wilk, L.; Nusair, M. Accurate Spin-Dependent Electron Liquid Correlation Energies for Local Spin-Density Calculations - A Critical Analysis. *Can. J. Phys.* **1980**, *58*, 1200–1211.
- (14) Schafer, A.; Horn, H.; Ahlrichs, R. Fully Optimized Contracted Gaussian-Basis Sets for Atoms Li to Kr. *J. Chem. Phys.* **1992**, *97*, 2571–2577.
- (15) Hehre, W. J.; Ditchfield, R.; Pople, J. A. Self-Consistent Molecular-Orbital Methods. XII. Further Extensions of Gaussian-Type Basis Sets for Use in Molecular-Orbital Studies of Organic-Molecules. *J. Chem. Phys.* **1972**, *56*, 2257–2261.
- (16) Hariharan, P. C.; Pople, J. A. Influence of Polarization Functions on Molecular-Orbital Hydrogenation Energies. *Theor. Chim. Acta* **1973**, *28*, 213–222.
- (17) Franch, M. M.; Pietro, W. J.; Hehre, W. J.; Binkley, J. S.; Gordon, M. S.; Defrees, D. J.; Pople, J. A. Self-Consistent Molecular-Orbital Methods. XXIII. A Polarization-Type Basis Set for Second-Row Elements. *J. Chem. Phys.* **1982**, *77*, 3654–3665.
- (18) McLean, A. D.; Chandler, G. S. Contracted Gaussian-Basis Sets for Molecular Calculations. I. Second Row Atoms, Z=11–18. *J. Chem. Phys.* **1980**, *72*, 5639–5648.
- (19) Krishnan, R.; Binkley, J. S.; Seeger, R.; Pople, J. A. Self-Consistent Molecular-Orbital Methods. XX. Basis Set for Correlated Wave-Functions. *J. Chem. Phys.* **1980**, *72*, 650–654.
- (20) Rulisek, L.; Jensen, K. P.; Lundgren, K.; Ryde, U. The reaction mechanism of iron and manganese superoxide dismutases studied by theoretical calculations. *J. Comput. Chem.* **2006**, *27*, 1398–1414.
- (21) Klamt, A.; Schuurmann, G. Cosmo - A New Approach to Dielectric Screening in Solvents with Explicit Expressions for the Screening Energy and Its Gradient. *J. Chem. Soc., Perkin Trans. 2* **1993**, 799–805.
- (22) Pack, G. R.; Loew, G. H. Semiempirical studies of the mechanism of models for the N-hydroxylation of amines by cytochrome P450. *Int. J. Quantum Chem.* **1979**, *16*, 381–390.
- (23) Rydberg, P.; Ryde, U.; Olsen, L. Sulfoxide, sulfur, and nitrogen oxidation and dealkylation by cytochrome P450. *J. Chem. Theory Comput.* **2008**, *4*, 1369–1377.
- (24) Li, C. S.; Wu, W.; Cho, K. B.; Shaik, S. Oxidation of Tertiary Amines by Cytochrome P450-Kinetic Isotope Effect as a Spin-State Reactivity Probe. *Chem.—Eur. J.* **2009**, *15*, 8492–8503.
- (25) Cho, K. B.; Moreau, Y.; Kumar, D.; Rock, D. A.; Jones, J. P.; Shaik, S. Formation of the active species of cytochrome P450 by using

iodosylbenzene: A case for spin-selective reactivity. *Chem.—Eur. J.* **2007**, *13*, 4103–4115.

(26) Roberts, K. M.; Jones, J. P. Anilinic N-Oxides Support Cytochrome P450-Mediated N-Dealkylation through Hydrogen-Atom Transfer. *Chem.—Eur. J.* **2010**, *16*, 8096–8107.

(27) Wang, Y.; Yang, C. L.; Wang, H. M.; Han, K. L.; Shaik, S. A new mechanism for ethanol oxidation mediated by cytochrome P450 2E1: Bulk polarity of the active site makes a difference. *Chembiochem* **2007**, *8*, 277–281.

(28) Kamachi, T.; Yoshizawa, K. A theoretical study on the mechanism of camphor hydroxylation by compound I of cytochrome P450. *J. Am. Chem. Soc.* **2003**, *125*, 4652–4661.

(29) Shaik, S.; Hirao, H.; Kumar, D. Reactivity patterns of cytochrome P450 enzymes: multifunctionality of the active species, and the two states-two oxidants conundrum. *Nat. Prod. Rep.* **2007**, *24*, 533–552.

(30) Rydberg, P.; Vasanthanathan, P.; Oostenbrink, C.; Olsen, L. Fast Prediction of Cytochrome P450 Mediated Drug Metabolism. *ChemMedChem* **2009**, *4*, 2070–2079.